Received: 2 January 2020 | Revised: 26 April 2020 | Accepted: 29 April 2020

DOI: 10.1111/bph.15099

RESEARCH PAPER

# Astaxanthin attenuates hepatic damage and mitochondrial dysfunction in non-alcoholic fatty liver disease by up-regulating the FGF21/PGC-1α pathway

Liwei Wu[1] | Wenhui Mo[2] | Jiao Feng[1] | Jingjing Li[1,3] | Qiang Yu[1] | Sainan Li[1] | Jie Zhang[1,4] | Kan Chen[1] | Jie Ji[1] | Weiqi Dai[1,3,5,6,7] | Jianye Wu[3] | Xuanfu Xu[2] | Yuqing Mao[8] | Chuanyong Guo[1]

[1]Department of Gastroenterology, Shanghai Tenth People's Hospital, Tongji University School of Medicine, Shanghai, China

[2]Department of Gastroenterology, Shidong Hospital of Shanghai, Shanghai, China

[3]Department of Gastroenterology, Putuo People's Hospital, Tongji University School of Medicine, Shanghai, China

[4]Shanghai Tenth Hospital, School of Clinical Medicine of Nanjing Medical University, Shanghai, China

[5]Department of Gastroenterology, Zhongshan Hospital of Fudan University, Shanghai, China

[6]Shanghai Institute of Liver Diseases, Zhongshan Hospital of Fudan University, Shanghai, China

[7]Shanghai Tongren Hospital, Shanghai Jiaotong University School of Medicine, Shanghai, China

[8]Department of Gastroenterology, Shanghai First People's Hospital, Shanghai Jiaotong University School of Medicine, Shanghai, China

**Correspondence**
Chuanyong Guo, Department of Gastroenterology, Shanghai Tenth People's Hospital, Tongji University School of Medicine, Shanghai 200072, China.
Email: guochuanyong@hotmail.com

Yuqing Mao Department of Gastroenterology, Zhongshan Hospital of Fudan University, Shanghai 200032, China; or Shanghai Institute of Liver Diseases, Zhongshan Hospital of Fudan University, Shanghai, 200032, China.
Email: maoyuqing198883@163.com

**Funding information**
the Health System Innovation Plan of Shanghai Putuo District Science and Technology Committee, Grant/Award Number: PTKWWS2018001; the Project of Shanghai Health Commission, Grant/Award Number: 2019469; the WBN Liver Disease Research Fund of China Hepatitis Prevention Foundation, Grant/Award Number: CFHPC2019031; theYangfan Plan of Shanghai Science and Technology Commission, Grant/Award Number: 2018YF1420000; Project of Shanghai Health Commission, Grant/Award Number: 2019469; Yangfan Plan of Shanghai

**Background and Purpose:** Non-alcoholic fatty liver disease (NAFLD) is considered to be one of the most common chronic liver diseases across worldwide. Astaxanthin (Ax) is a carotenoid, and beneficial effects of astaxanthin, including anti-oxidative, anti-inflammatory, and anti-tumour activity, have been identified. The present study aimed to elucidate the protective effect of astaxanthin against NAFLD and its underlying mechanism.

**Experimental Approach:** Mice were fed either a high fat or chow diet, with or without astaxanthin, for up to 12 weeks. L02 cells were treated with free fatty acids combined with different doses of astaxanthin for 48 h. Histopathology, expression of lipid metabolism, inflammation, apoptosis, and fibrosis-related gene expression were assessed. And the function of mitochondria was also evaluated.

**Key Results:** The results indicated that astaxanthin attenuated HFD- and FFA-induced lipid accumulation and its associated oxidative stress, cell apoptosis, inflammation, and fibrosis both in vivo and in vitro. Astaxanthin up-regulated FGF21 and PGC-1α expression in damaged hepatocytes, which suggested an unrecognized mechanism of astaxanthin on ameliorating NAFLD.

**Conclusion and Implications:** Astaxanthin attenuated hepatocyte damage and mitochondrial dysfunction in NAFLD by up-regulating FGF21/PGC-1α pathway. Our

**Abbreviations:** ALT, alanine aminotransferase; AST, aspartate aminotransferase; FFA, free fatty acid; HFD, high-fat diet; NAFLD, non-alcoholic fatty liver disease; NAS, NAFLD activity score; NASH, non-alcoholic steatohepatitis; NRF1, nuclear respiratory factor 1; OXPHOS, oxidative phosphorylation; PGC-1α, PPAR-γ coactivator-1α; TFAM, mitochondrial transcription factor A; TGs, triglycerides; ΔΨm, mitochondrial membrane potential.

Liwei Wu and Wenhui Mo contributed equally to this work and share the same first authorship.

  

Science and Technology Commission, Grant/Award Number: 2018YF1420000; WBN Liver Disease Research Fund of China Hepatitis Prevention Foundation, Grant/Award Number: CFHPC2019031; Health System Innovation Plan of Shanghai Putuo District Science and Technology Committee, Grant/Award Number: PTKWWS2018001; National Natural Science Foundation of Shanghai, Grant/Award Number: 19ZR1447700; National Natural Science Foundation of China, Grant/Award Numbers: 81670472, 81700502, 81800538

results suggest that astaxanthin may become a promising drug to treat or relieve NAFLD.

**What is already known**

- Astaxanthin can exert beneficial effects in various diseases.
- FGF21 is involved in a number of metabolic pathways, including lipid metabolism.

**What this study adds**

- Astaxanthin achieved its anti-NAFLD effects by up-regulating the FGF21/PGC-1α pathway.
- OATP1A/1B and CYP3A contribute to the elimination of larotrectinib.

**What is the clinical significance**

- Astaxanthin may become a promising drug to treat or relieve NAFLD in the near future.

## 1 | INTRODUCTION

Non-alcoholic fatty liver disease (NAFLD) arises from the imbalance of hepatic free fatty acid (FFA) metabolism and is considered one of the most common chronic liver diseases with a prevalence of approximately 25%–30% worldwide (Ahmed et al., 2017). NAFLD has a wide disease spectrum, ranging from simple steatosis, non-alcoholic steatohepatitis (NASH), liver fibrosis, cirrhosis, and hepatocellular carcinoma. NAFLD pathogenesis has been is described as the two-hit process. The first hit is triggered by an overload of fatty acids and triglycerides (TGs) in liver. The second hit is characterized as chronic stress, including the generation of ROS, exacerbated pro-inflammatory responses, enhanced lipid peroxidation, and endoplasmic reticulum stress associated with fatty liver (Chen, Yu, Xiong, Du, & Zhu, 2017; Day & James, 1998). However, the underlying mechanisms remain poorly understood.

According to the "two-hit" theory, the second hit involves the mitochondria as the main target (Baker & Friedman, 2018). The mitochondrion, whose shape is highly variable, contains a double membrane structure and is the primary location of ATP production and the main source of ROS (Li et al., 2018),. Mitochondria play an important regulatory role in many cellular activities, such as oxidative stress, cell apoptosis and gene expression. Excessive intracellular lipid deposition promotes oxidative stress reactions to produce excessive amounts of ROS, which results in mitochondrial dysfunction and cytotoxicity. This promotes a vicious cycle and exacerbates the development of NAFLD (Zhou et al., 2018).

The growth factor FGF21 is an endocrine member of the FGF family, and it is involved in a variety of metabolic systems. Circulating FGF21 is largely derived from the liver, and its levels are highly correlated with hepatic function (Badman et al., 2007). In addition, clinical studies have shown that FGF21 is associated with fatty liver disease (Hu et al., 2019; Li et al., 2010). Animal experiments have shown that FGF21 mRNA is increased in the livers of mice with NAFLD (Badman et al., 2007). Studies with FGF21 gene knockout or overexpressing mice have shown that FGF21 plays an important role in lipid metabolism (Yan et al., 2015). **PPAR-γ coactivator-1α (PGC-1α)**, an important transcriptional coactivator, is a central inducer of mitochondrial biosynthesis and energy metabolism (Lustig et al., 2011; Yan et al., 2013). Convincing evidence has shown that FGF21 can regulate PGC-1α (Fisher et al., 2012; Potthoff et al., 2009).

Astaxanthin is a carotenoid that exists in shrimp, crab, salmon, algae, and other marine organisms, which exhibits both hydrophilic and lipotropic properties (Ambati, Phang, Ravi, & Aswathanarayana, 2014). And has a molecular structure that allows it to directly enter cells and quench active oxygen and free radicals, allowing it to act as naturally occurring antioxidant, with an antioxidant activity 500 times greater than that of vitamin E (Ambati et al., 2014; Ni et al., 2015). Astaxanthin is known to protect mitochondria by preventing oxidative stress (Baburina et al., 2019) and, with good safety data (Brendler & Williamson, 2019; Williamson, Liu, & Izzo, 2020), astaxanthin exhibits a wide range of beneficial effects (Ambati et al., 2014), including anti-inflammatory and anti-tumour activities. More relevantly, astaxanthin reduced lipid accumulation and induced energy expenditure in mice on a high-fat diet (HFD) (Jia, Wu, Kim, Kim, & Lee, 2016; Kim et al., 2017).

In this study, we have evaluated the effects of astaxanthin in C57BL/6 mice fed an HFD, which is a widely used animal model (Recena Aydos et al., 2019), and investigated its underlying mechanisms. Our results clearly show that astaxanthin administration up-

regulated FGF21 and PGC-1α, resulting in the prevention of HFD-induced fatty liver, effects which were associated with the regulation of mitochondrial function. Our data suggest that astaxanthin can be considered a potential agent for treating fatty liver.

## 2 | METHODS

### 2.1 | Cell culture and treatment

The normal human liver cell line, LO2 cells, was purchased from the Chinese Academy of Science Committee Type Culture Collection Cell Bank (RRID:CVCL_6926). The cells were cultured in h-DMEM supplemented with 10% FBS, 100 U·ml$^{-1}$ of penicillin, and 100 g·ml$^{-1}$ of streptomycin in a humidified incubator at 37°C in 5% $CO_2$. Oleic acid (OA) and palmitic acid (PA) were dissolved in 5% BSA. LO2 cells were exposed to an FFA mixture of 800-μM OA and 400-μM PA for 48 h to induce steatosis. Cells were treated with 30-, 60-, and 90-μM astaxanthin. After eliminating other factors (Supporting Information), the cells were divided into five groups: (1) control group, treated only with 5% BSA; (2) FFA group, treated with an FFA mixture for 48 h; (3) FFA + Ax30 group, treated with 30-μM astaxanthin and the FFA mixture described above; (4) FFA + Ax60 group, treated with 60-μM astaxanthin and the FFA mixture described above; and (5) FFA + Ax90 group, treated with 90-μM astaxanthin and the FFA mixture described above.

### 2.2 | Plasmid construction, lentivirus packaging, and cellular transfection

FGF21 overexpression (FGF21-oe) or knockdown (sh-FGF21) lentivirus was synthesized and cloned into the LV5 (EF-1aF/GTP&Puro) and LV3 (H1/GTP&Puro) vector by GenePharma Biotechnology (Shanghai, China). Empty vectors (EV5 and EV3) were used as controls.

To establish a stable lentivirus transfection, L02 cell line, L02 cells were seeded into 24-well plates. When the cells had reached 60%–70% confluency, they were transfected with EV5, FGF21-oe, EV3, or sh-FGF21 lentivirus with 5 μg·ml$^{-1}$ of polybrene for 24 h. The positive cells were selected by puromycin, and the transfection efficiency was determined by qPCR and Western blot.

### 2.3 | CCK8 assay

L02 cells were plated at a density of 5 × 10$^4$ cells·ml$^{-1}$ into 96-well plates (100 μl medium per well) with five replicates. The L02 cells were then treated with different concentrations of astaxanthin and FFA. After incubation for 48 h, cell viability was measured using a CCK8 assay according to the manufacturer's instructions.

### 2.4 | Animal experiments and design

All animal care and experimental protocols complied with the guidelines of the China National Institutes of Health and were approved by the Animal Care and Use Committee of Shanghai Tongji University, China.. All efforts were made to minimize suffering of experimental mice in this research. Animal studies are reported in compliance with the ARRIVE guidelines (Kilkenny, Browne, Cuthill, Emerson, & Altman, 2010) and with the recommendations made by the British Journal of Pharmacology.

Male C57 (RRID:IMSR_ORNL:C57BL/Rl) mice (20 g ± 0.5 g) were bought from Shanghai SLAC Laboratory Animal Co., Ltd. (Shanghai, China) and were housed under controlled temperatures, humidity, and lighting with ad libitum food and water. The experimental design was based on earlier work (Liu et al., 2019; Mao et al., 2015; Monmeesil, Fungfuang, Tulayakul, & Pongchairerk, 2019). The mice were randomly distributed into the following six groups:

1 Control group (*n* = 7): mice were fed a standard chow diet (CD).
2 HFD group (*n* = 7): mice were fed an HFD and received saline by gavage every 2 days in later 10 weeks.
3 HFD + Ax group (n = 7): mice were fed an HFD and received 10, 30, and 60 mg·kg$^{-1}$ of astaxanthin by gavage every 2 days in later 10 weeks.
4 Negative group (*n* = 7): mice were fed an HFD and received a tail-vein injection of control-siRNA eight times during the first 4 weeks.
5 siRNA-FGF21 group (*n* = 7): mice were fed an HFD and received a tail-vein injection of FGF21-siRNA eight times during the first 4 weeks.
6 siRNA-FGF21 + Ax group(*n* = 7): mice were fed an HFD and received a tail-vein injection of FGF21-siRNA eight times during first 4 weeks and received 60 mg·kg$^{-1}$ of astaxanthin by gavage every 2 days during the later 10 weeks.

Astaxanthin was dissolved in saline.

Body weight and food intake were measured each week. Mice were killed after 12 weeks, and the serum and liver tissues were collected for further analysis. Blinding was used in the subsequent analyses.

### 2.5 | In vivo transfection with FGF21 siRNA

Firstly, siRNA FGF21 (guide: 5′GAAGCCGGGAGUUAUUCAATT3′, passenger: 5′UUGAAUAACUCCCGGCUUCTT3′) or siRNA control (GenePharma, Shanghai, China) was dissolved in RNase-free water to a final concentration of 1 μg·μl$^{-1}$. Next, FGF21 siRNA or negative control siRNA and Entranster-in vivo transfection reagent (Engreen, Co., Beijing, China) were mixed and diluted with 10% glucose following the manufacturer's instructions. Then, 20 μl of the diluted mixture were injected in the tail vein of mice.

## 2.6 | Oil Red O staining

L02 cells were plated into six-well plates and exposed to FFA with or without Ax for 48 h. After fixation with 4% paraformaldehyde for 10 min, fixed cells were stained in Oil Red O solution for 15 min, and then their nucleus was stained by haematoxylin for 3 min.

## 2.7 | Histological and immunohistochemistry analysis

Liver tissue samples, which were fixed in 4% paraformaldehyde, were embedded with paraffin. Serial sections were sliced at 5 μm and stained with haematoxylin–eosin (H&E) and Masson's trichrome to observe the damage. Oil Red O staining was used to visualize lipid droplets in the liver.

The antibody-based procedures used in this study comply with the recommendations made by the *British Journal of Pharmacology* (Alexander et al., 2018). For immunohistochemistry (IHC) staining, the slices were dewaxed and rehydrated, and after an antigen retrieval process and blocking, they were incubated with primary antibodies overnight. For the terminal deoxynucleotidyl transferase dUTP nick end labelling (TUNEL) assay, the slices were treated ccording to the instruction and then incubated in the TUNEL reaction mixture at room temperature for 1 h. The brown-stained cells were regarded as TUNEL-positive cells. All of the images were captured by an optical microscope (DM6B, Leica, Hamburg, Germany). The primary antibodies used were listed in Table 1.

## 2.8 | Immunofluorescence analysis

L02 cells were seeded onto glass cover slips in six-well plates and treated with FFA and astaxanthin for 48 h, washed with cold PBS, and fixed in 4% paraformaldehyde in PBS at room temperature. The fixed cells were washed three times with PBS and kept in chilled methanol for 10 min at −20°C. The cells were washed three times and incubated with the primary antibody (listed in Table 1) and secondary antibody (Alexa Fluor goat anti-mouse 488, 1:500). Then, the nucleus was counter-stained blue with DAPI and mounted with anti-fluorescence quenching sealant. The slips were imaged using an inverted fluorescence microscope (IX53, Olympus, Tokyo, Japan.

## 2.9 | Annexin V-FITC/PI double staining

L02 cells ($5 \times 10^5$) were plated into 12-well plates and treated with FFA and Ax for 48 h. The cells were then washed and trypsinized and resuspended in 500-μl binding buffer containing Annexin V (5 μl) and PI (5 μl). The cells were further incubated for 30 min at 4°C, in the dark. The samples were analysed by flow cytometry (BD Biosciences).

## 2.10 | Measurement of intracellular ROS

The ROS assay kit was bought from Beyotime to test the production of intracellular ROS. The cells ($5 \times 10^5$) were pretreated with FFA and astaxanthin for 48 h, collected, and resuspended in serum-free medium containing 10-μM DCFH-DA. The collected cells were cultured in 37°C for 20 min and were immediately measured by flow cytometry.

## 2.11 | Measurement of the mitochondrial membrane potential (ΔΨm)

The changes in MMP were measured by MMP assay kit with JC-1 (Beyotime). The cells were pretreated with FFA and astaxanthin for 48 h and resuspended and then incubated with JC-1 for 20 min in

**TABLE 1** Primer antibodies used in the study

| Antibody | Dilution ratio | Supplier | Catalogue Number | RRID |
|---|---|---|---|---|
| β-actin | 1/1000 | Proteintech | 60008-1-Ig | AB_2289225 |
| TNF-α | 1/1000 | Cell Signaling Technology | 11948 | AB_2687962 |
| IL-1β | 1/1000 | Cell Signaling Technology | 12242 | AB_2715503 |
| iNOS | 1/1000 | Cell Signaling Technology | 13120S | AB_2687529 |
| Bax | 1/2000 | Proteintech | 23931-1-AP | AB_2833256 |
| Caspase 9 | 1/1000 | Proteintech | 66169-1-Ig | AB_2833257 |
| α-SMA | 1/1000 | Proteintech | 14395-1-AP | AB_2223009 |
| TGF-β1 | 1/1000 | Proteintech | 21898-1-AP | AB_2811115 |
| ColI | 1/1000 | Proteintech | 14695-1-AP | AB_2082037 |
| FGF21 | 1/1000 | abcam | ab 171941 | AB_2629460 |
| PGC-1α | 1/1000 | abcam | ab54481 | AB_881987 |
| OXPHOS | 1/250 | mitoscience | MS604 | AB_2629281 |

37°C. After measuring by flow cytometry, the fluorescence intensity was analysed.

## 2.12 | Quantitative real-time PCR for the mtDNA content

The total DNA was extracted from cells or frozen liver samples using a QIaamp DNA mini kit (QIAGEN, Valencia, CA). The DNA concentration was determined using a PicoGreen DNA quantitation kit (Molecular Probes, Eugene, OR). The sequences for mouse cytochrome β and β-actin are presented in Table S1. Primers and an FAM-labelled TAMRA-quenched probe were ordered from TaKaRa Biotechnology. The amplification and quantitation of mtDNA was accomplished using a PCR detection kit (DRR039A, TaKaRa).

## 2.13 | Determining ATP content

The cellular ATP levels were measured using an ATP bioluminescent assay kit (Beyotime, China). The assay was carried out in accordance with the manufacturer's instruction.

## 2.14 | Biochemical analysis

After keeping blood samples at 4°C overnight, serum was separated by centrifugation at 4600 x *g* for 10 mins and stored at −80°C. Cultured cells were trypsinized and collected for further analysis. Serum and cultured cells were collected. The aspartate aminotransferase (AST), alanine aminotransferase (ALT), and triglyceride (TG) levels were determined using commercially available kits (Jiancheng Co. Nanjing, China). The assays were carried out according to the manufacturer's protocols.

## 2.15 | Expression of FGF21 protein

Blood samples were collected from the mice, and the plasma was isolated. Circulating FGF21 was measured using an ELISA kit purchased from Jonln Bioscience (Shanghai, China). The cell culture medium was collected, and the level of FGF21 protein expression was measured using an ELISA kit obtained from Huyu Bioscience (Shanghai, China). Both ELISAs were conducted following the manufacturer's protocol.

## 2.16 | Real-time quantitative PCR

The total RNA was isolated from the cells and tissues according to the standard protocol. The first strand of cDNA was synthesized using a reverse transcription kit (TaKaRa Biotechnology) and was used to analyse the indicator expression. The primers used in the PCR reactions are listed in Table 2. Real-time PCR experiments were performed according to the protocol of the real-time PCR kit (Takara, Otsu, Shiga, Japan). The ratio of each gene compared to β-actin was calculated by standardizing the ratio of each control to the unit value.

## 2.17 | Western blotting

Protein was extracted from cultured cells or frozen liver samples. A total of 30- or 80-ng protein was loaded onto 7.5%, 10%, and 12.5% SDS-polyacrylamide gels, and the separated proteins were transferred to PVDF or NC membranes. The membranes were incubated overnight at 4°C with primary antibodies (listed in Table 1) followed by an incubation with a secondary antibody(1:2,000). Finally, the blots were scanned using an Odyssey two-colour infrared laser imaging system (Li-Cor, Lincoln, NE, USA).

## 2.18 | Co-immunoprecipitation assay

Cells were seeded into 10-cm dishes and then treated with FFA and astaxanthin for 48 h. A co-immunoprecipitation (Co-IP) assay was performed using a Pierce Co-immunoprecipitation Kit (Thermo Scientific, Waltham, MA, USA) according to the manufacturer's protocol. Primary antibodies used are listed in Table 1. The IP antibody against FGF21 was from Santa Cruz (sc-81946, RRID:AB_2104609).

## 2.19 | Electron microscopy

After prefixing, the tissues were washed six times with potassium phosphate (0.1 M, pH 7.4) and then fixed with 2% osmium tetroxide. Samples were then dehydrated and embedded with pure epoxy resin. Mitochondria were observed by electron microscopy (JEM-1230 from JEOL, Tokyo, Japan). Images were acquired and handled with the Image J analysis software.

## 2.20 | NAFLD activity score evaluation

To assess morphological changes in liver, we used the NAFLD activity score (NAS) system for evaluation, which has been defined as the sum of scores for steatosis(0–3), lobular inflammation (0–3), and hepatocellular ballooning (0–2). Samples with scores more than 5 were associated with a diagnosis of NASH and scores less than 3 were diagnosed as not NASH.

## 2.21 | Data and statistical analysis

The data and statistical analysis comply with the recommendations of the *British Journal of Pharmacology* on experimental design and analysis in pharmacology (Curtis et al., 2018). Statistical analysis was

**TABLE 2** Sequences of primer pairs used for amplification of mRNA by real-time PCR

| For mice | | For human | |
|---|---|---|---|
| β-actin | F GTGACGTTGACATCCGTAAAGA | β-actin | F CTGGAACGGTGAAGGTGACA |
| | R GCCGGACTCATCGTACTCC | | R AAGGGACTTCCTGTAACAATGCA |
| BAX | F AGACAGGGGCCTTTTTGCTAC | BAX | F AAGAAGCTGAGCGAGTGT |
| | R AATTCGCCGGAGACACTCG | | R GGAGGAAGTCCAATGTC |
| IL-1β | F CGATCGCGCAGGGCTGGGCGG | — | |
| | R AGGAACTGACGGTACTGATGGA | | |
| iNOS | F CTCACTGGGACAGCACAGAA | — | |
| | R GATGTGGCCTTGTGGTGAA | | |
| TNF-α | F CAGGCGGTGCCTATGTCTC | — | |
| | R CGATCACCCCGAAGTTCAGTAG | | |
| APOB | F GCTCAACTCAGGTTACCGTGA | APOB | F TGCTCCACTCACTTTACCGTC |
| | R AGGGTGTACTGGCAAGTTTGG | | R TAGCGTCCAGTGTGTACTGAC |
| ApoE | F CTCCCAAGTCACACAAGAACTG | ApoE | F GTTGCTGGTCACATTCCTGG |
| | R CCAGCTCCTTTTTGTAAGCCTTT | | R GCAGGTAATCCCAAAAGCGAC |
| ADRP | F CTTGTGTCCTCCGCTTATGTC | ADRP | F ATGGCATCCGTTGCAGTTGAT |
| | R GCAGAGGTCACGGTCTTCAC | | R GGACATGAGGTCATACGTGGAG |
| FAT/CD36 | F ATGGGCTGTGATCGGAACTG | FAT/CD36 | F GGCTGTGACCGGAACTGTG |
| | R TTTGCCACGTCATCTGGGTTT | | R AGGTCTCCAACTGGCATTAGAA |
| CPT1α | F TGGCATCATCACTGGTGTGTT | CPT1α | F TCCAGTTGGCTTATCGTGGTG |
| | R GTCTAGGGTCCGATTGATCTTTG | | R TCCAGAGTCCGATTGATTTTTGC |
| FATP5 | F TCTATGGCCTAAAGTTCAGGCG | FATP5 | F TGGAGGAGATCCTTCCCAAGC |
| | R CTTGCCGCTCTAAAGCATCC | | R TGGTCCCCGAGGTATAGATGAA |
| FGF21 | F GTGTCAAAGCCTCTAGGTTTCTT | FGF21 | F CTGTGGGTTTCTGTGCTGG |
| | R GGTACACATTGTAACCGTCCTC | | R CCGGCTTCAAGGCTTTCAG |
| FOXA1 | F ACATTCAAGCGCAGCTACCC | FOXA1 | F GCAATACTCGCCTTACGGCT |
| | R TGCTGGTTCTGGCGGTAATAG | | R TACACACCTTGGTAGTACGCC |
| PGC-1a | F TATGGAGTGACATAGAGTGTGCT | PGC-1a | F TCTGAGTCTGTATGGAGTGACAT |
| | R GTCGCTACACCACTTCAATCC | | R CCAAGTCGTTCACATCTAGTTCA |
| PPAR-α | F AACATCGAGTGTCGAATATGTGG | PPAR-α | F ATGGTGGACACGGAAAGCC |
| | R CCGAATAGTTCGCCGAAAGAA | | R CGATGGATTGCGAAATCTCTTGG |
| SREBP-1c | F TTGTGGAGCTCAAAGACCTG | SREBP-1c | F ACAGTGACTTCCCTGGCCTAT |
| | R TGCAAGAAGCGGATGTAGTC | | R GCATGGACGGGTACATCTTCAA |
| Tm6sf2 | F GATCACCTACGACCCTCTCTATG | Tm6sf2 | F GCATTGATGAGCGCCCTAATC |
| | R TGGAGTGCAATGACAAGGTCC | | R AGTGGGTCATAGGAGACCTCG |
| UCP1 | F GTGAACCCGACAACTTCCGAA | UCP1 | F AGGTCCAAGGTGAATGCCC |
| | R TGCCAGGCAAGCTGAAACTC | | R TTACCACAGCGGTGATTGTTC |
| Caspase 9 | F GGCTGTTAAACCCCTAGACCA | Caspase 9 | F CTTCGTTTCTGCGAACTAACAGG |
| | R TGACGGGTCCAGCTTCACTA | | R GCACCACTGGGGTAAGGTTT |
| Collagen I | F TTCACCTACAGCACGCTTGT | — | |
| | R TCTTGGTGGTTTTGTATTCGATGA | | |
| α-SMA | F CCCAGACATCAGGGAGTAATGG | — | |
| | R TCTATCGGATACTTCAGCGTCA | | |
| TGF-β1 | F CCTGCAAGACCATCGACATG | — | |
| | R GAGCCTTAGTTTGGACAGGATCTG | | |
| CTGF | F CGCCAACCGCAAGATTG | — | |
| | R ACACGGACCCACCGAAGAC | | |

undertaken only when each group size has a minimum of $n$ = 5 independent samples/individuals, and in a blinded manner. We used unpaired two-tailed Student's $t$ test or one-way ANOVA with the Tukey's post hoc test, while post hoc tests were conducted only if $F$ achieved $P < 0.05$ and there was no significant variance inhomogeneity. A $P$ value below 0.05 ($P < 0.05$) was considered to be significantly different, and $P$ value is not varied later in Section 3. Outliers in our experiments were included in the data analysis and presentation. To control of the unwanted sources of variation, normalization of the data was also carried out. For data that did not pass normality testing, log transformation was applied to generate Gaussian-distributed data set that could be subjected to parametric statistical analysis or non-parametric statistics were used (Wilcoxon rank sum test or Kruskal–Wallis H test). Data were presented as mean ± SEM, and all statistical analyses were performed using GraphPad Prism v6.02 software (GraphPad Software, USA).

2.22Materials

High-glucose DMEM (h-DMEM), FBS, penicillin, and streptomycin were obtained from Gibco (Thermo Fisher Scientific, Waltham, MA, USA). Astaxanthin, BSA, oleic acid (OA), and palmitic acid (PA) were purchased from Sigma-Aldrich (St. Louis, MO, USA). HFD (D12492) was composed of 20% protein, 60% fat, and 20% carbohydrate of the caloric intake; 5.24 kcal·g−1 was purchased from Shanghai QF Biosciences (Shanghai, China). Cell Counting Kit (CCK-8) was obtained from Yeasen Biotechnology (Shanghai, China). Annexin V-FITC apoptosis detection kit and PI/RNase Staining Buffer were purchased from BD Biosciences (San Jose, CA, USA). Oligonucleotide primers were produced in Generay Biotech (Shanghai, China). The PrimeScript RT Reagent kit and SYBR Premix Ex Taq were obtained from TaKaRa Biotechnology (Dalian, China). Details for primary antibodies used in our experiments were listed in Table 1.

## 2.22 | Nomenclature of targets and ligands

Key protein targets and ligands in this article are hyperlinked to corresponding entries in http://www.guidetopharmacology.org, the common portal for data from the IUPHAR/BPS Guide to PHARMACOLOGY (Harding et al., 2018), and are permanently archived in the Concise Guide to PHARMACOLOGY 2019/20 (Alexander, Cidlowski, et al., 2019; Alexander, Fabbro et al., 2019a, 2019b; Alexander, Kelly et al., 2019a, 2019b).

# 3 | RESULTS

## 3.1 | Astaxanthin alleviated hepatic damage in mice fed an HFD by regulating lipid metabolism, fibrosis, and inflammation

We established an HFD-induced fatty liver model to determine the effect of astaxanthin in non-alcoholic fatty liver, and the time-course of the experiments is shown in Figure 1a. To confirm the control group, we compared the natural control, vehicle, astaxanthin-treated, and negative group, and the results were showed in Figure 2s. Thus, vehicle, astaxanthin, and si-NC did not cause observable damage to mice. During these 12 weeks, food intake were recorded each week, and no significant differences were observed in the average food intake among the control, HFD, and astaxanthin-treated groups (Figure 1b). The body weight of the mice was measured twice a week, and Figure 1c shows that

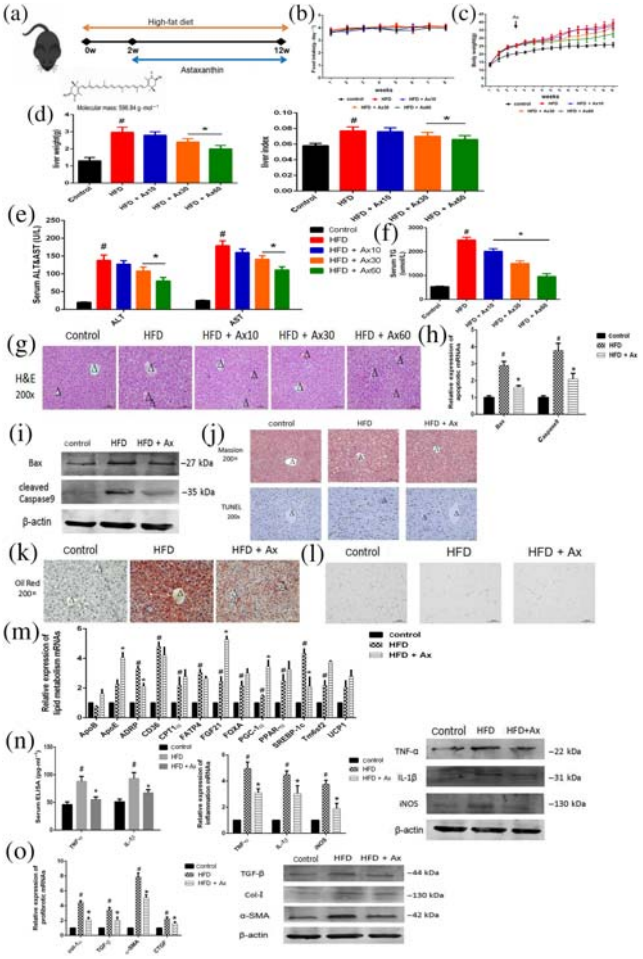


**FIGURE 1** Astaxanthin (Ax) alleviated hepatic damage in mice fed with HFD by regulating lipid metabolism, fibrosis, and inflammation. (a) Experimental flow chart; (b) food intake; (c) body weight; (d) liver weight and liver index; (e) serum ALT and AST levels; (f) serum TG levels; (g) H&E staining (×200) of livers (positive cells were marked by arrows; central veins were marked as Δ); (h) Relative expression of apoptotic mRNA; (i) Expression of apoptotic proteins; (j) Masson staining and TUNEL staining (×200) of livers (central veins were marked as Δ); (k) Oil Red O staining (×200) of livers (central veins were marked as Δ); (l) H&E staining (×200) of WAT; (m) Relative expressions of lipogenesis-related genes in livers; (n) Serum ELISA levels of TNF-α and IL-1β and expression of mRNA and protein levels of inflammatory genes; (o) Expression of mRNA and protein levels of profibrotic genes. Data shown are means ± SEM; n = 7 in each group. $^{\#}P$<.05, significantly different from control, $^{*}P$<.05, significantly different from HFD

treatment with astaxanthin reduced the weight gain caused by the HFD. Figure 1d demonstrated that the mice treated with astaxanthin had a lower liver weight compared with the HFD group. Different groups with different doses showed different effects and the body and liver weight changes were most pronounced in the highest dose group. The levels of serum ALT and AST are presented in Figure 1e. Long-term HFD caused an elevation of ALT and AST, which could be reduced by astaxanthin in a dose-dependent manner. Another biochemical quantitative determination showed that astaxanthin prevented the dyslipidaemia induced by HFD (Figure 1f). Pathological changes in the liver of these mice were assessed every 4 weeks, and these results were shown in Figure S2. The H&E stained samples shown in Figure 1g showed that the mice fed an HFD for 12 weeks displayed the typical appearance of hepatic fatty acid infiltration, which suggested that fat metabolism was disrupted. We also observed infiltration of inflammatory cells and ballooning in the samples. However, treatment with astaxanthin effectively alleviated these symptoms. And similar to the above, all of these changes were dose-dependent, and the group treated with 60 $mg{\cdot}kg^{-1}$ astaxanthin showing the greatest effects.

We used NAS to evaluate morphological changes in liver (Table 3). NAS scores of HFD group were significantly higher than control group, and Ax treatment down-regulated them strikingly. Based on these analyses, we selected the dose of 60 $mg{\cdot}kg^{-1}$ for our further in vivo studies.

TUNEL staining exhibited HFD toxicity in the liver, and additional positive sites were observed in the model group compared with the control group. Astaxanthin treatment reduced the observed toxicity. In addition, the level of **Bax** and **caspase 9** mRNA and protein expression confirmed the above results (Figure 1h–j). Increased expression of Bax and caspase 9 in the model group was reversed by treatment with astaxanthin. Thus, we ensured the beneficial effect of Ax in NAFLD.

NAFLD involves multiple mechanisms, including altered lipid metabolism, dysregulation of cytokine production, inflammation, oxidative stress, and fibrosis. The samples stained with Oil Red O, in Figure 1k, revealed that the size and content of lipid droplets were small and reduced in the astaxanthin group, which indicated alleviation of hepatic lipid deposition. Moreover, astaxanthin reduced the enlargement of adipocytes caused by HFD in WAT (Figure 1l), suggesting that, to some degree, astaxanthin could regulate lipid metabolism in both the liver, and the entire body. Hepatic mRNA expression of lipid metabolism-related genes were detected and the results are shown in Figure 1m. These genes included those for ApoB, ApoE, ADRP, **CD36**, CPT1α, **FATP5**, FGF21, FOXA, PGC-1α, SREBP-1c, Tm6sf2, and **UCP1**, which reflected FFA synthesis, decomposition and transportation. Our data showed that astaxanthin administration significantly inhibited fatty acid uptake, blocked fatty acids synthesis and increased lipid decomposition and fatty acid oxidation. Astaxanthin treatment significantly reduced the secretion of inflammatory cytokines and relieved hepatic inflammation. The level of TNF-α, IL-1β, and iNOS

**TABLE 3** NAFLD activity scores (NAS) used to evaluate morphological changes in the experimental groups

| Parameters | Control | HFD | HFD + Ax10 | HFD + Ax30 | HFD + Ax60 | Negative | HFD + FGF(−) | HFD + FGF(−) + Ax |
|---|---|---|---|---|---|---|---|---|
| Steatosis (0–3) | 0.20 ± 0.45 | 2.14 ± 0.69$^{\#}$ | 2.01 ± 0.48 | 1.84 ± 0.38 | 1.43 ± 0.53$^{*}$ | 0.29 ± 0.49 | 2.43 ± 0.53$^{\&}$ | 1.86 ± 0.69$^{\%,+}$ |
| Lobular inflammation (0–3) | 0.00 ± 0.00 | 1.85 ± 0.69$^{\#}$ | 1.69 ± 0.48 | 1.49 ± 0.48$^{*}$ | 1.42 ± 0.53$^{*}$ | 0.14 ± 0.38 | 2.28 ± 0.49$^{\&}$ | 1.71 ± 0.49$^{\%,+}$ |
| Hepatocellular ballooning (0–2) | 0.00 ± 0.00 | 1.71 ± 0.49$^{\#}$ | 1.67 ± 0.53 | 1.52 ± 0.53 | 1.14 ± 0.69$^{*}$ | 0.14 ± 0.38 | 1.85 ± 0.38 | 1.43 ± 0.53$^{\%}$ |
| NAS | 0.20 ± 0.45 | 4.57 ± 0.77$^{\#}$ | 4.34 ± 0.69 | 3.81 ± 0.63$^{*}$ | 3.57 ± 0.53$^{*}$ | 0.43 ± 0.53 | 5.14 ± 0.53$^{\&}$ | 4.43 ± 0.79$^{\%,+}$ |

Data shown are means ± SD; $n$=7 per group. $^{\#}P < .05$, significantly different from control; $^{*}P < .05$, significantly different from HFD; $^{+}P < .05$, significantly different from HFD + Ax60; $^{\&}P < .05$, significantly different from Negative; $^{\%}P < .05$, significantly different from HFD + FGF(−).

expression was assessed by ELISA, qRT-PCR, and Western blot. The expression of these pro-inflammatory cytokines was increased in the model group but decreased following astaxanthin treatment (Figure 1n). As shown in Figure 1j, HFD caused almost no fibre formation. However, in the model group, the level of hepatic collagen I, TGF-β1, α-SMA, and CTGF expression were substantially up-regulated compared with the control group; and astaxanthin induced a decrease (Figure 1o). It was concluded that astaxanthin had protected the liver of NAFLD mice by regulating altered lipid metabolism, fibrosis, and inflammation.

### 3.2 | Astaxanthin suppressed FFA-induced injury in hepatocytes

To further study the beneficial mechanism(s) of astaxanthin in FLD, we treated the L02 cell line with FFAs to establish an in vitro model. We treated the cells with different doses of FFAs and astaxanthin for 48 h and measured the effects using an CCK8 assay (Figure 2a). From these results, we found the beneficial effects of astaxanthin were concentration-dependent over the range of 30 - 90 μM, with the best effect at 90 μM. Thus, in

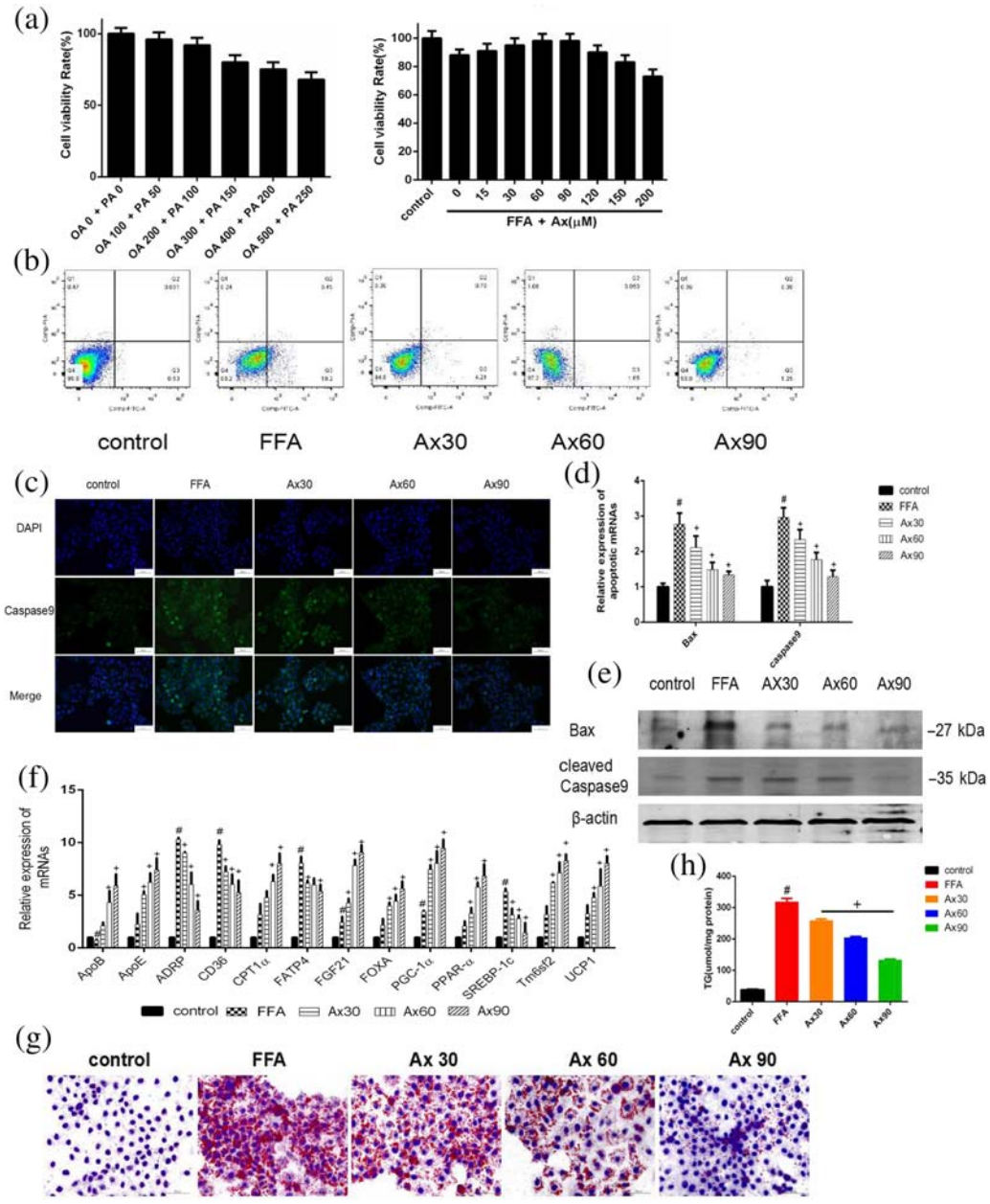


**FIGURE 2** Astaxanthin (Ax) suppressed FFAs-induced injury in hepatocytes. (a) CCK8 assay; (b) flow cytometry for apoptosis; (c) immunofluorescence for caspase 9 (×200); (d) relative expression of apoptotic mRNA; (e) expression of apoptotic proteins; (f) relative expressions of lipogenesis related genes in hepatocytes; (g) Oil Red O staining of hepatocytes (×200); (h) cellular TG levels. Data were presented as mean ± SEM; n = 5 in each group. $^{\#}P<.05$, significantly different from control, $^{+}P<.05$, significantly different from FFA

subsequent work, we used astaxanthin at 30, 60, and 90 μM. The proportion of living and dead cells was determined by flow cytometry, and the results (Figure 2b) showed that incubation with the FFAs induced approximately 20% cell death, and astaxanthin improved the cell survival rate by about 18%. We also measured the expression of Bax and caspase 9. As shown in Figure 2c–e, Bax and caspase 9 were up-regulated by exposure to FFAs and this effect was inhibited by astaxanthin. The protective effects of astaxanthin on Bax and caspase 9 were also concentration-dependent. The results of staining with Oil Red O (Figure 2g) and assay of TG (Figure 2h) showed that exposure to astaxanthin clearly reduced the lipid concentration in FFA-loaded L02 hepatocytes, concentration-dependently. The changes in the genes related to lipid metabolism in Figure 2f were similar to those in Figure 1k. These results demonstrated clearly that astaxanthin protected L02 hepatocytes against FFA-induced injury.

### 3.3 | The beneficial role of astaxanthin was associated with the regulation of mitochondrial function

As mitochondrial dysfunction plays an important role in the progression of NAFLD, we explored changes in mitochondrial function in our model sytem. Oxidative phosphorylation (OXPHOS) is an important indicator of mitochondrial function and we measured changes in OXPHOS expression by Western blot (Figure 3a,b). OXPHOS complexes were reduced when FFAs were loaded both in vivo and in vitro, and treatment with astaxanthin restored the OXPHOS enzymic activity. This indicated that astaxanthin improved mitochondrial biogenesis and function. Compared with the control group, the level of mitochondrial ROS production was elevated by FFA loading and reduced concentration-dependently by treatment with astaxanthin (Figure 3e). As mitochondria are the major site of ATP production, we examined

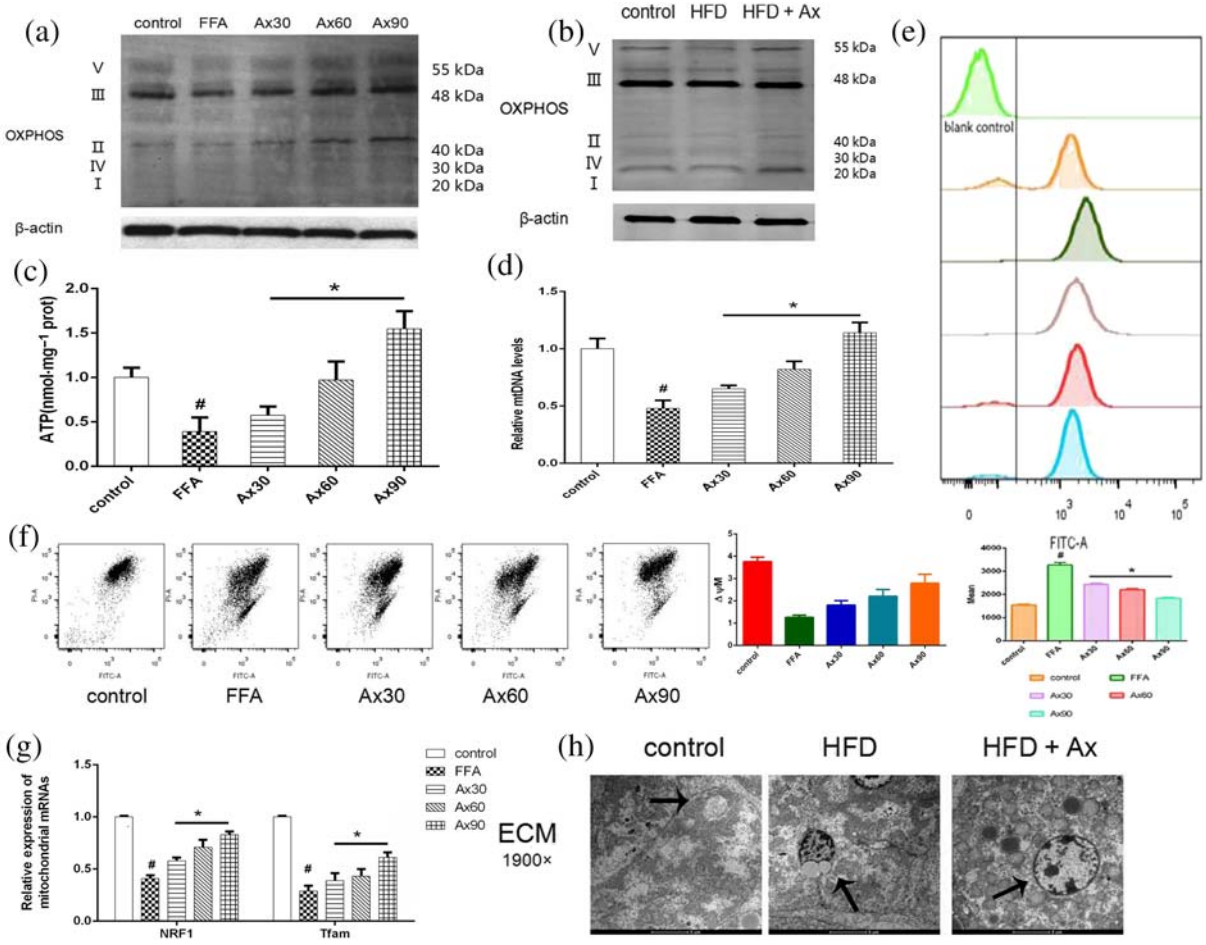


**FIGURE 3** The beneficial effects of treatment with astaxanthin (Ax) was associated with its regulation of mitochondrial function. (a,b) OXPHOS expression of hepatocytes and livers; (c) ATP levels; (d) relative mtDNA levels; (e) ROS analysed by flow cytometry; (f) mitochondrial membrane potential (MMP) analysed by flow cytometry; (g) relative expression of mitochondrial mRNAs (NRF1 and TFAM); (h) mitochondria under electron microscopy (×1900) (mitochondria were marked by arrows). Data shown are means ± SEM; in (b), $n = 7$; $n = 5$ in other groups. $^{\#}P<.05$, significantly different from control, $^{*}P<.05$. significantly different from FFA

the energy production in FFA-loaded cells using a luciferase-based ATP assay kit. As expected, FFAs reduced ATP production, and the addition of astaxanthin improved ATP generation (Figure 3c). The graph in Figure 3d shows that the number of mtDNA copies, which were associated with mitochondrial biogenesis, was decreased by FFA and significantly increased by astaxanthin, concentration-dependently. We also found that when loaded with FFAs, the mitochondrial membrane potential (ΔΨm) was dissipated. However, astaxanthin restored the ΔΨm in a concentration-dependent manner (Figure 3f). Moreover, astaxanthin markedly elevated the expression of nuclear respiratory factor 1 (NRF1) and mitochondrial transcription factor A (TFAM) in hepatocytes, which were reduced by FFA loading (Figure 3g). Changes in the mitochondrial morphology were observed by electron microscopy (Figure 3h). In addition to lipid droplets, we observed some lipid inclusions in the mitochondria after FFA loading, along with increased mitochondrial swelling, cristae disorder, and matrix particles.

### 3.4 | FGF21/PGC-1α was the target of astaxanthin, and the beneficial effects of astaxanthin were influenced by the overexpression or knockdown of FGF21 in vitro

Based on the results of genes related to lipid metabolism and the repor7ted beneficial effects of FGF21 already mentioned, astaxanthin described above were likely to be closely related to FGF21 and PGC-1α, so we decide to assess expression of FGF21 in our system. We measured the level of circulating FGF21 protein in the serum of our mice (Figure 4a), and found that the serum FGF21 was increased in the HFD-fed mice. In addition, administration of astaxanthin aggravated this increase. The level of FGF21 gene and protein expression was detected by qRT-PCR and Western blot both in vivo and in vitro, and consistent results were obtained (Figure 4b). Treatment with astaxanthin up-regulated FGF21 expression dose-dependently. The immunohistochemical and immunofluorescence results in Figure 4c,d exhibited the same changes. Thus, FGF21 appeared to be involved in the beneficial effects of astaxanthin in NAFLD models.

After screening the valid sequences (Figure S3), lentiviruses containing PKM2-oe, PKM2-ko, or an empty vector were transfected into L02 cells. The transfection results were shown by green fluorescent imaging, qRT-PCR, and Western blot in Figure 4e–g, which confirmed a successful transfection. It has been reported that FGF21 interacts with PGC-1α and promotes the transcription of genes downstream from PGC-1α. The unified expression of FGF21 and PGC-1α detected by Western blot and qRT-PCR in above figures suggested that Ax treatment may have a positive effect on the interaction between FGF21 and PGC-1α. We conducted a Co-IP assay to assess the relationship between astaxanthin, FGF21, and PGC-1α in L02 cells (Figure 4h). The results showed that PGC-1α was pulled-down by FGF21, and the level of the FGF21/PGC-1α complex was increased following astaxanthin treatment.

The actions of FGF21/PGC-1α alone and any synergistic action with astaxanthin in both animals and cell models were then determined. Figure 4i shows the levels of TG. Figure 4j shows the staining

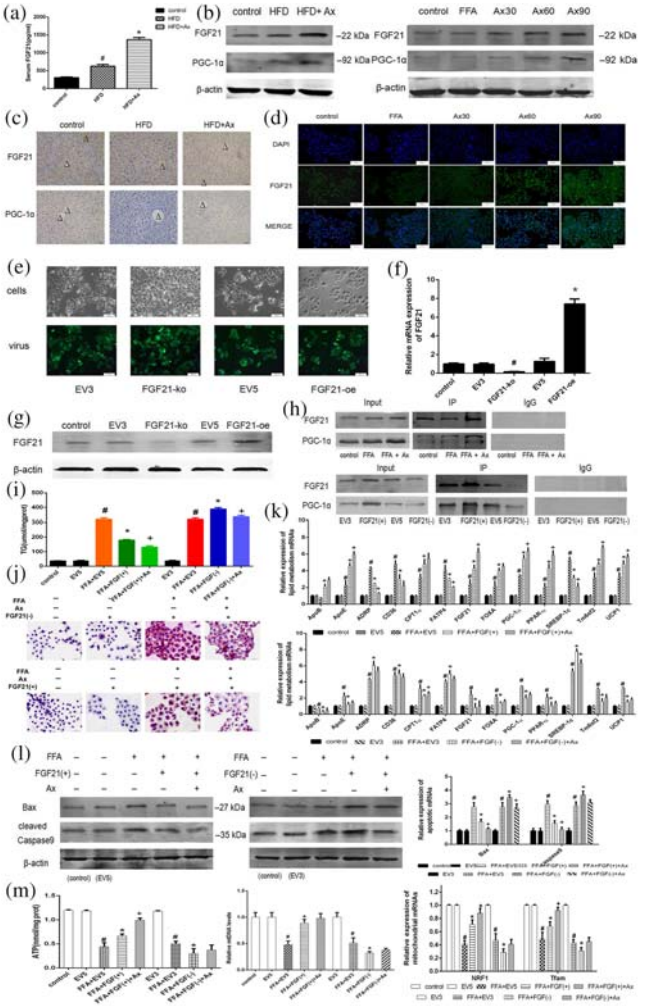

**FIGURE 4** FGF21/PGC-1α was the target of astaxanthin (Ax) and the beneficial effects of astaxanthin treatment were influenced by the overexpression or knockdown of FGF21 in vitro. (a) Serum FGF21 levels. Data shown are means ± SEM. $^{\#}P < .05$, significantly different from control, $^{*}P < .05$, significantly different from HFD. (b) Protein levels of FGF21 and PGC-1α of liver and hepatocytes; (c) IHC for FGF21 and PGC-1α (×200) (central veins were marked as Δ); (d) immunofluorescence for FGF21 (×200); (e) transfection results of L02 cells (×200); (f) Relative FGF21 mRNA expression of transfected cells. Data shown are means ± SEM. $^{\#}P < .05$, significantly different from EV3; $^{*}P < .05$, significantly different from EV5; (g) FGF21 protein expression of transfected cells; (h) CO-IP assay of FGF21 and PGC-1α; (i) cellular TG levels; (j) Oil Red O staining of transfected cells (×200); (k) relative expressions of lipogenesis related genes of transfected cells; (l) expression of mRNA and protein levels of apoptotic genes; (m) ATP levels, relative mtDNA levels, and relative expression of mitochondrial mRNAs. Data shown are means ± SEM. $^{\#}P < .05$, significantly different from EV; $^{*}P<.05$, significantly different from FFA+EV; $^{+}P<.05$, significantly different from FFA + FGF(+/−). In (a–c), $n = 7$ in each group; in (d–m), $n = 5$ in each group

by Oil Red O of transfected L02 cells, and Figure 4k showed the level of mRNA expression of some genes involved in lipid metabolism. Overall, these results show that FFA accumulation in FGF21(−) cells was significantly higher than that in FGF21(+) cells. The efficacy of

astaxanthin in regulating lipid metabolism was decreased in FGF21(–) cells, but enhanced in FGF21(+) cells. We also measured the changes in apoptosis in these transfected cells (Figure 4l). Changes caused by astaxanthin in the gene and protein expression of the markers for apoptosis in FGF21(–) cells were minor whereas they were very clear in FGF21(+) cells. Thus, we assumed the protective effect of astaxanthin against hepatocyte damage, was suppressed in FGF21(–) cells. Therefore, FGF21 may be the target of astaxanthin when this compound has its beneficial effects. Furthermore, we assayed mitochondrial biogenesis and function in the transfected L02 cells with or without the treatment of FFA and astaxanthin. The results for ATP, mtDNA, and mRNA (Figure 4m) suggest that the influence of astaxanthin on the mitochondria were dependent, to a large extent, on the presence of FGF21.

In addition, Figure 6a shows the effects on cell apoptosis. As anticipated, the protective effects of astaxanthin on hepatocytes loaded with FFAs were suppressed by FGF21 down-regulation. Figure 6b illustrates the intracellular deposition of FFAs and these its results were consistent. Thus, the beneficial effect of astaxanthin in reducing lipid toxicity was blocked by the down-regulation of FGF21.

## 3.5 | The down-regulation of FGF21 aggravated liver damage in HFD-fed mice

We injected FGF21 siRNA into the tail veins of mice to down-regulate FGF21 expression and administered astaxanthin and the effects are shown in Figure 5a. An ELISA and Western blot were performed to confirm the effect of the siRNA (Figure 5b,c). Food intake was also recorded (Figure 5d) and no differences were observed between HFD, FGF21(–), and astaxanthin-treated groups. The body weight of these mice were recorded twice a week and Figure 5e shows that the down-regulation of FGF21 induced serious weight gains, which were reversed by astaxanthin treatment . Figure 5f shows that mice with lower FGF21 expression had a heavier liver. The results of the serum ALT, AST, and TG assays are given in Figure 5g,h. During the long-term HFD, the down-regulated FGF21 expression appeared to increase the liver enzyme index. H&E and Oil Red O staining in Figure 5i,j showed that the FGF21(–) group of mice exhibited a more severe hepatic fatty infiltration, which was only slightly improved in the astaxanthin-treated group. Hepatic mRNA expression of lipid metabolism-associated genes (Figure 5k) showed changes consistent with the results already described. In addition, we assessed the inflammatory response, cell apoptosis, and fibrosis progression among these three groups (Figure 5l–n). The HFD led to more serious injury in the livers of the FGF21(–) group of mice, and astaxanthin could occasionally reduce the damage induced by FGF21 down-regulation. The graph of Table 3 showed the same results. Figure 5o shows morphological changes in the mitochondria observed by electron microscopy. In the FGF21(–) group, lipid droplets in hepatocytes were clearly visible. Pleomorphic mitochondria, increased matrix particles, and membrane rupture were also observed.

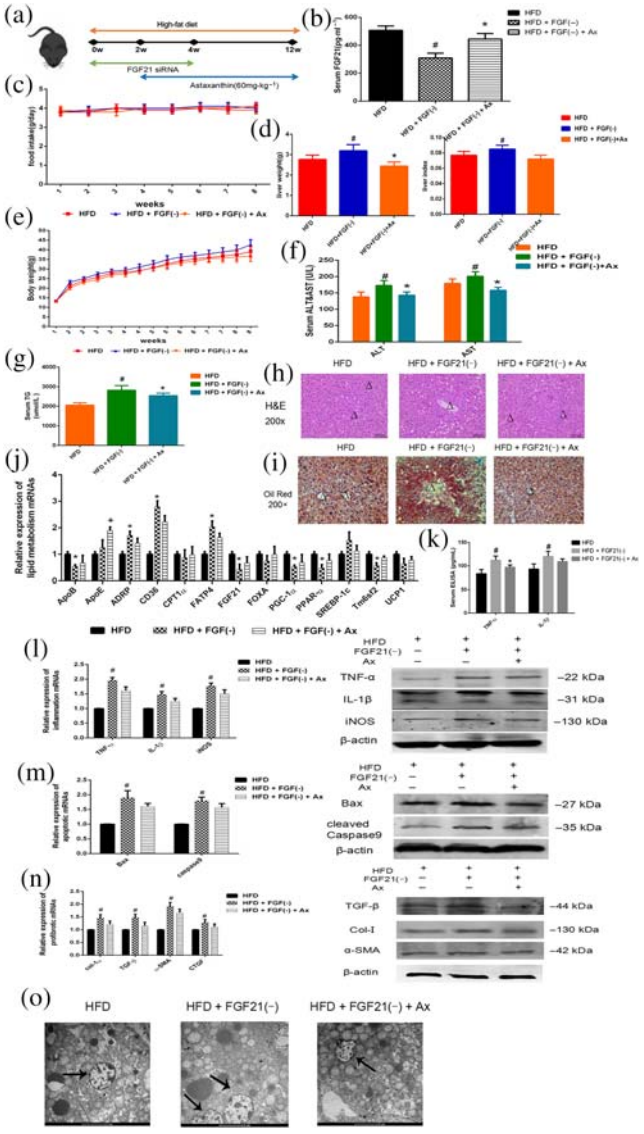


**FIGURE 5** FGF21 down-regulation aggravated liver damage in HFD-fed mice. (a) Experimental flow chart; (b) serum FGF21 levels; (c) food intake; (d) liver weight and liver index; (e) bodyweight; (f) serum ALT and AST levels; (g) serum TG levels; (h) H&E staining (×200) of livers (central veins were marked as Δ); (i) Oil Red O staining (×200) of livers (central veins were marked as Δ); (j) relative expressions of lipogenesis related genes in livers; (k) Serum ELISA levels of TNF-α and IL-1β; (l) expression of mRNA and protein levels of inflammatory genes; (m) Expression of mRNA and protein levels of apoptotic genes; (n) Expression of mRNA and protein levels of profibrotic genes; (o) mitochondria under electron microscopy (×1900) (mitochondria were marked by arrows). Data shown are means ± SEM; $n = 7$ in each group. $^{\#}P<.05$, significantly different from HFD; $^{*}P<.05$, significantly different from HFD + FGF(–)

Further, we compared and summarized the experimental results with or without FGF21 gene down-regulation and found that the effects of astaxanthin were claerly inhibited by such down-regulation. The morphological observations under the microscope (Figure 6c) and serum examination (Figure 6e) showed that the hepatic pathology of the FGF21(–) mice treated with astaxanthin was significantly more

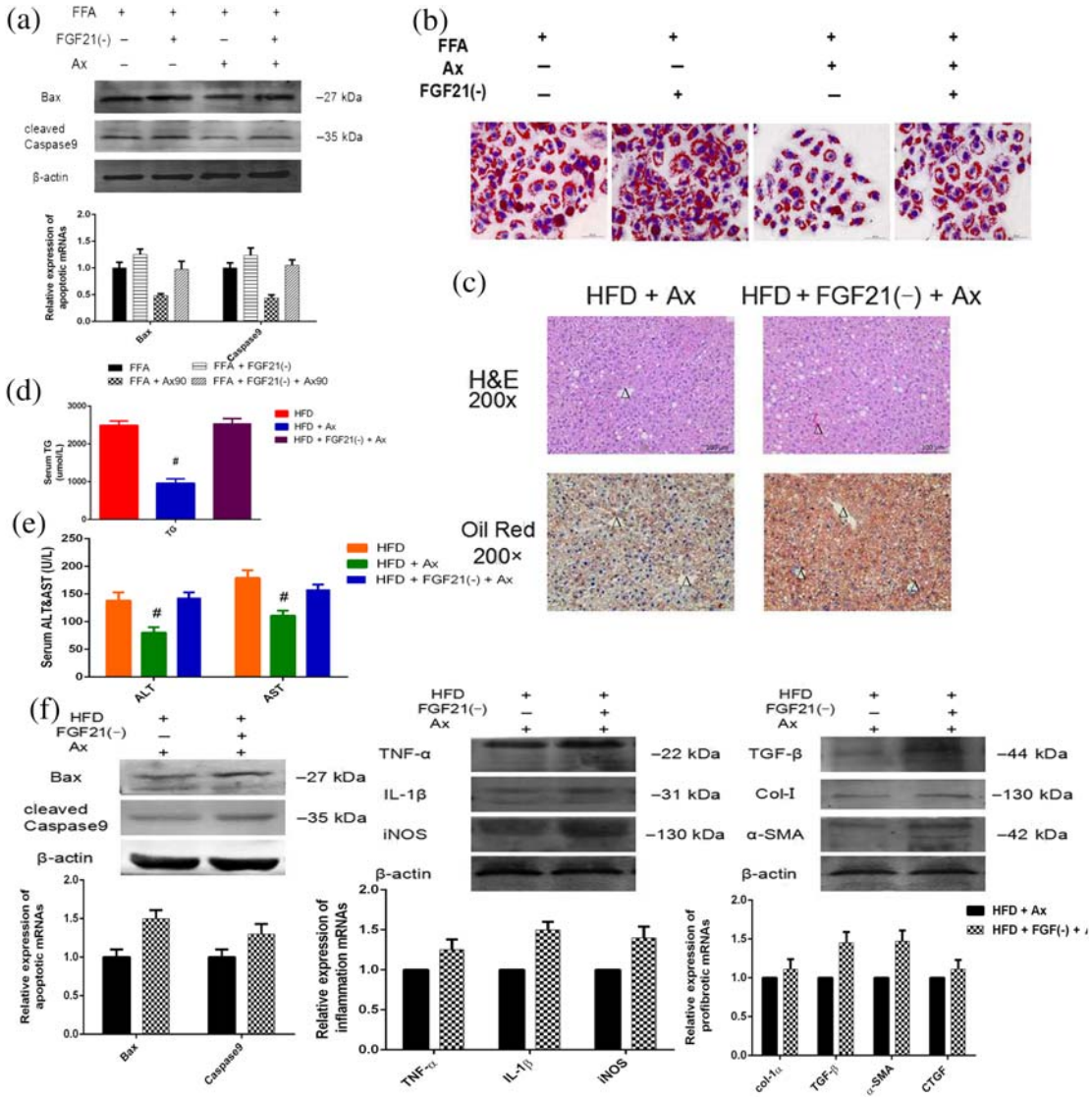


**FIGURE 6** The protective effect of astaxanthin (Ax) was decreased by FGF21 down-regulation. (a) H&E staining (×200) and Oil Red O staining (×200) of livers (central veins were marked as Δ); (b) serum ALT and AST levels; (c) serum TG levels; (d) expression of mRNA and protein levels of inflammatory, apoptotic, and profibrotic genes of liver; (e) expression of mRNA and protein levels of apoptotic genes of transfected cells; (f) Oil Red O staining of transfected cells (×200). Data shown are means ± SEM; $n = 7$ in each group. $^{\#}P<.05$, significantly different from HFD

serious. Figure 6f summarises a comparison among these groups regarding the states of inflammation, apoptosis, and fibrosis. Table 3 shows the comparison between HFD + Ax and siFGF21 + HFD + Ax group. The protective effects of astaxanthin were reduced by the deficiency of FGF21.

## 4 | DISCUSSION

NAFLD is a clinicopathological syndrome characterized by bullous steatosis of the liver. Although NAFLD is now a worldwide health concern, the full pathogenesis leading up to lipid accumulation, cell apoptosis, inflammation, and fibrosis remains ill defined. Many nutri-based compounds have been assessed for antioxidant properties in the treatment of NAFLD, such as L-carnitine (Montesano et al., 2019), chrysin (Pai, Munshi, Panchal, Gaur, & Juvekar, 2019), and plumbagin (Pai et al., 2019). Consequently, many scientists agree that nutrigenomic aspects are very important in the management of NAFLD.

At the same time, ample evidence suggests the involvement of astaxanthin in the protection of liver function of liver disease. Several articles reported the mechanisms underlying astaxanthin treatment of NAFLD injury. Jia et al. (2016) showed that astaxanthin activated **PPAR-α** while inhibiting **PPAR-γ**, thus reducing lipid accumulation in hepatocytes, and its function was also related to the inhibition of **Akt–mTOR**–autophagy pathway. But they did not analyse the underlying mechanisms in detail (Jia et al., 2016). Besides, Kim et al. (2017) confirmed that astaxanthin could regulate fatty acid oxidation and mitochondrial biogenesis, leading to inhibition of inflammation and fibrosis in obese mice. However, our knowledge of the the mechanism(s) of astaxanthin in NAFLD is still inadequate.

To some extent, elevated serum TG levels and weight gain are typical manifestations of NAFLD and are often accompanied by an increase in the liver index. ALT and AST are typical indicators of liver injury, and they can reveal the damaged state of liver cells, in most cases. Our HFD-fed mice showed significant elevation of these liver enzymes and such increased levels were decreased following astaxanthin treatment. The characteristic histological feature of NAFLD is the accumulation of fat in hepatocytes. The results of Oil Red O staining showed that treatment with astaxanthin alleviated the formation of lipid droplets. Consistent with the results of food intake, astaxanthin treatment did not inhibit HFD-induced weight gain. Combining the qPCR results of lipid metabolism genes, the effects of astaxanthin in inhibiting excessive fat deposition was through altering lipid metabolism.

The pathogenesis of NAFLD is considered to be a complex multifactorial process. Inflammation, cell apoptosis, and fibrogenesis are all typical damage-associated changes seen in the NAFLD model and are caused by the lipotoxicity (Garcia-Monzón et al., 2000; Kumar et al., 2019). We next assessed changes in the liver from both in vivo and in vitro models. Inflammation is one of the hallmarks of lipid toxicity in the liver, and **TNF-α**, **IL-1β** and **iNOS** are all involved in the inflammatory response induced by lipids (Chen, Yu, et al., 2017; Sharma et al., 2013; Tilg, Moschen, & Szabo, 2016) and are secreted by damaged hepatocytes. By sectioning the livers and measuring the expression of TNF-α, IL-1β, and iNOS, we found astaxanthin reversed inflammation in the pathogenic processes of NAFLD. Apoptosis is one of the main manifestations of poorly stimulated cells (Czabotar, Lessene, Strasser, & Adams, 2014). The abnormal expression of apoptosis is strongly linked to the progression of NAFLD, and apoptosis abduction is one theory of lipid toxicity (Schwabe & Luedde, 2018). After observing TUNEL-stained and measuring the expression of Bax and caspase 9, we found that astaxanthin ameliorated the occurrence of apoptosis in NAFLD. Moreover, fibrosis is a required pathological feature when defining NASH (Miele, Forgione, Gasbarrini, & Grieco, 2007; Schuppan, Surabattula, & Wang, 2018). The expression of fibrosis marker genes exhibited a marked increase in the liver of these NAFLD mice and was significantly decreased by astaxanthin administration. These data indicate that astaxanthin reversed HFD diet-induced hepatic fibrosis. Taken together, astaxanthin alleviated the liver damage caused by lipid toxicity in NAFLD. This was consistent with previous research results.

Mitochondrial dysfunction plays a central role in the pathophysiology of NASH because it affects hepatic lipid homeostasis and promoting ROS production, lipid peroxidation, cytokine release, and cell death (Kelly & Scarpulla, 2004; Wang et al., 2015). In turn, excessive ROS then aggravates OXPHOS impairment and mitochondrial dysfunction (Bailey et al., 2005; Begriche, Igoudjil, Pessayre, & Fromenty, 2006). Therefore, we measured changes in mitochondrial function. Enzymic activities involved in OXPHOS were reduced in both in vivo and in vitro experimental models, resulting in a reduction of ATP generation. The decreased mitochondrial DNA in the model groups was in line with the changes in ROS, OXPHOS, and ATP. Treatment with astaxanthin substantially restored OXPHOS complexes and ATP levels, reduced ROS production, and increased the mtDNA copy number, which suggested amelioration of mitochondrial biogenesis and function. In addition, we examined the levels of NRF1 and TFAM transcription, as NRF1 has been associated with the initiation of mitochondrial biogenesis by activating gene transcription for mitochondrial proteins, including TFAM (Scarpulla, 2008; Virbasius & Scarpulla, 1994). After translocating into mitochondria, TFAM launches the transcription and replication of mtDNA (Kang, Kim, & Hamasaki, 2007). Therefore, astaxanthin may act as an effective treatment for NASH by modulating mitochondrial dysfunction.

To confirm the function of astaxanthin in regulating lipid metabolism, we measured various lipid metabolism-related genes, including those for ApoB, ApoE, ADRP, CD36, CPT1α, FATP5, FGF21, FOXA, PGC-1α, SREBP-1c, Tm6sf2, and UCP1. Among these, ApoB, ApoE, CD36, and FATP5 are involved in fatty acid transportation; CPT1α and UCP1 are associated with β-oxidation; and ADRP, FGF21, FOXA, PGC-1α, Tm6sf2, and SREBP-1c for lipid synthesis and degradation. Our study of these genes has shown that astaxanthin administration significantly increased lipid efflux and degradation and fatty acid oxidation, while blocking cholesterol and fatty acids synthesis, as well as fatty acid uptake. In analysing the data, we found that the variation of FGF21 expression was significant and stable. Combined with its physiological characteristics, it is possible that astaxanthin inhibited NAFLD progression through regulating FGF21.

FGF21 is involved in glucose metabolism, lipid metabolism, and insulin resistance (Piccinin & Moschetta, 2016; Potthoff, 2017). The C-terminus of FGF21 binds to b-Klotho (KLB) with a high affinity and forms a complex with **FGF receptors (FGFRs)** on the surface of cells (Chen et al., 2017; Kharitonenkov et al., 2008). Therefore, the co-expression of FGFRs and KLB determines the tissue specificity of FGF21 and FGF21 is highly expressed in the liver, adipose tissue and pancreas of mice (Kharitonenkov et al., 2008; Agrawal et al., 2018). In the context of NASH pathology, deficiency of FGF21 markedly exacerbated the TG accumulation in the liver, which is due to the impaired fatty acid oxidation, increased fatty acid uptake, and enhanced inflammation and fibrosis. Additionally, increased levels of FGF21, due to endogenous or exogenous factors, can stimulate glucose uptake, increase insulin sensitivity, decrease serum glucose and lipid levels, and elevate energy expenditure (Fisher & Maratos-Flier, 2016; Gimeno & Moller, 2014).

The co-regulator PGC-1α modulates lipid metabolism in various tissues (Boström et al., 2012; Gallardo-Montejano et al., 2016) and also plays a significant role in liver diseases (Liu et al., 2016; Piccinin, Villani, & Moschetta, 2019). Leone et al. (2005) isolated hepatocytes from PGC-1α-deficient mice and found that both the fatty acid oxidation and mitochondrial respiration rates were diminished. Our results showed that astaxanthin greatly enhanced the level of FGF21 and PGC-1α mRNA and protein expression. The Co-IP results suggested that there may be direct or indirect interactions between FGF21 and PGC-1α. According to the hypothesis associated with the development of NAFLD, mitochondria modulate OXPHOS and ROS generation, thereby affecting hepatic lipid homeostasis. Many studies have shown that the regulation of mitochondrial function is closely related to FGF21 (Lehtonen et al., 2016) and PGC-1α (Gallardo-Montejano et al., 2016). Therefore,

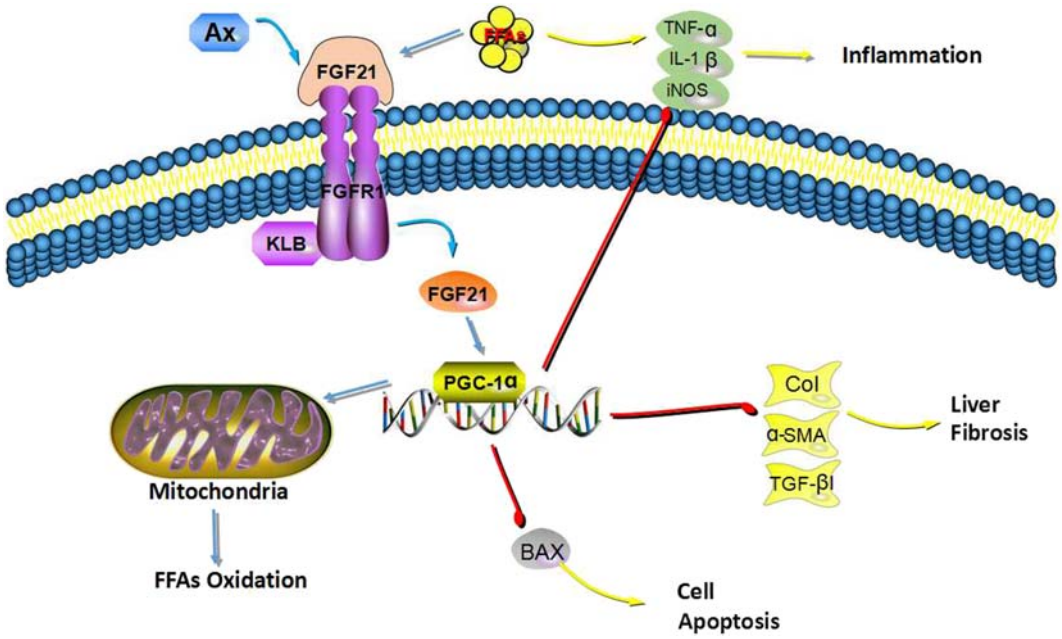


**FIGURE 7** Mechanisms underlying our results. Astaxanthin (Ax) decreased the severity of experimental steatohepatitis via mechanisms likely to involve the up-regulation of FGF21/PGC-1α. Treatment with astaxanthin substantially ameliorated mitochondrial biogenesis and functionality by restoring the OXPHOS complexes and ATP levels, which reduced ROS production and increased the mtDNA copy number. Thus, astaxanthin alleviated inflammation, cell apoptosis and fibrosis induced by lipid overload

the protective functions of astaxanthin against fatty liver diseases may at least partly depend on its regulation of FGF21/PGC-1α.

To test our hypothesis, FGF21 was overexpressed or silenced, via lentivirus transfection in L02 cells. Also, FGF21 siRNA was administered to mice to sustain low levels of FGF21, in vivo. We collected the samples and used the same method as described previously to conduct various tests and analyses. As expected, FGF21 expression exhibited a close relationship with lipid accumulation, the inflammatory response, fibrosis and apoptosis. Low levels of FGF21 led to aggravated HFD- or FFA-induced hepatocyte injury, which was relieved by FGF21 overexpression. Moreover, by comparing the effects of astaxanthin under different states of FGF21 expression, the down-regulation of FGF21 suppressed the effects of astaxanthin on HFD- or FFA-induced hepatocyte injury, which indicated that FGF21 was tightly related to the function of astaxanthin in inhibiting lipid accumulation, inflammation, fibrosis, and cell apoptosis. Besides, after the expression of FGF21 changed, PGC-1α expression also changed accordingly. We have concluded that astaxanthin could act as an FGF21 agonist to up-regulate the FGF21/PGC-1α system to inhibit the progression of fatty liver disease. This represents a previously unrecognized mechanism of astaxanthin in ameliorating HFD-induced fatty liver. Moreover, it should be noted that no death or signs of toxicity were observed for 12 weeks of astaxanthin administration. As the potential toxicity of FGF21 in skeletal homeostasis has been indicated in previous studies (Kharitonenkov & DiMarchi, 2015), this side effect can be greatly mitigated by astaxanthin.

In conclusion, we have demonstrated that astaxanthin prevented hepatic TG accumulation in mice fed an HFD and in the L02 cell line treated with FFAs, and alleviated inflammation, cell apoptosis, and fibrosis induced by lipids. Treatment with astaxanthin substantially ameliorated mitochondrial biogenesis and functionality by restoring the OXPHOS complexes and ATP levels, which reduces ROS production and increases the mtDNA copy number. Astaxanthin decreased the severity of experimental steatohepatitis via mechanisms likely to involve the up-regulation of FGF21/PGC-1α. Our studies confirmed that astaxanthin may become a promising drug to treat or relieve NAFLD (Figure 7).

## ACKNOWLEDGEMENTS

This work was supported by the National Natural Science Foundation of China (No. 81670472, 81700502, and 81800538); National Natural Science Foundation of Shanghai (No. 19ZR1447700); the Health System Innovation Plan of Shanghai Putuo District Science and Technology Committee (no. PTKWWS2018001); the WBN Liver Disease Research Fund of China Hepatitis Prevention Foundation (No. CFHPC2019031); the Yangfan Plan of Shanghai Science and Technology Commission (No. 2018YF1420000); the Project of Shanghai Health Commission (No. 2019469).

## AUTHOR CONTRIBUTIONS

The authors' contributions are as follows: conceptualization, L.W., W.M.; methodology, L.W., J.F. and J.L.; software, J.J. and Y.M.; validation, K.C., S.L., J.J. and J.Z.; formal analysis, L.W., W.D. and S.L.; investigation, L.W., W.D. and K.C.; writing original draft preparation, L.W.; writing review and editing, Y.M.,J.F. and W.M; visualization, L.W; supervision, C.G.; funding acquisition, J.W., J.L., X.X., Y.M. and C.G.

## CONFLICT OF INTEREST

The authors have declared that no competing interest exists.

## DECLARATION OF TRANSPARENCY AND SCIENTIFIC RIGOUR

This Declaration acknowledges that this paper adheres to the principles for transparent reporting and scientific rigour of preclinical research as stated in the BJP guidelines for Design & Analysis, Immunoblotting and Immunochemistry, and Animal Experimentation, and as recommended by funding agencies, publishers and other organisations engaged with supporting research.

## ORCID

*Chuanyong Guo* https://orcid.org/0000-0002-6527-4673

## REFERENCES

Agrawal, A., Parlee, S., Perez-Tilve, D., Li, P., Pan, J., Mroz, P. A., … DiMarchi, R. D. (2018). Molecular elements in FGF19 and FGF21 defining KLB/FGFR activity and specificity. *Mol Metab*, *13*, 45–55. https://doi.org/10.1016/j.molmet.2018.05.003

Ahmed, M. H., Noor, S. K., Bushara, S. O., Husain, N. E., Elmadhoun, W. M., Ginawi, I. A., … Almobarak, A. O. (2017). Non-alcoholic fatty liver disease in Africa and Middle East: An attempt to predict the present and future implications on the healthcare system. *Gastroenterology Research*, *10*, 271–279. https://doi.org/10.14740/gr913w

Alexander, S. P. H., Cidlowski, J. A., Kelly, E., Mathie, A., Peters, J. A., Veale, E. L., … CGTP Collaborators. (2019). THE CONCISE GUIDE TO PHARMACOLOGY 2019/20: Nuclear hormone receptors. *British Journal of Pharmacology*, *176*, S229–S246. https://doi.org/10.1111/bph.14750

Alexander, S. P. H., Fabbro, D., Kelly, E., Mathie, A., Peters, J. A., Veale, E. L., … CGTP Collaborators. (2019a). THE CONCISE GUIDE TO PHARMACOLOGY 2019/20: Catalytic receptors. *British Journal of Pharmacology*, *176*, S247–S296. https://doi.org/10.1111/bph.14751

Alexander, S. P. H., Fabbro, D., Kelly, E., Mathie, A., Peters, J. A., Veale, E. L., … CGTP Collaborators. (2019b). THE CONCISE GUIDE TO PHARMACOLOGY 2019/20: Enzymes. *British Journal of Pharmacology*, *176*, S297–S396. https://doi.org/10.1111/bph.14752

Alexander, S. P. H., Kelly, E., Mathie, A., Peters, J. A., Veale, E. L., Faccenda, E., … CGTP Collaborators. (2019a). THE CONCISE GUIDE TO PHARMACOLOGY 2019/20: Other Protein Targets. *British Journal of Pharmacology*, *176*, S1–S20. https://doi.org/10.1111/bph.14747

Alexander, S. P. H., Kelly, E., Mathie, A., Peters, J. A., Veale, E. L., Armstrong, J. F., … CGTP Collaborators. (2019b). THE CONCISE GUIDE TO PHARMACOLOGY 2019/20: Transporters. *British Journal of Pharmacology*, *176*, S397–S493. https://doi.org/10.1111/bph.14753

Alexander, S. P., Roberts, R. E., Broughton, B. R., Sobey, C. G., George, C. H., Stanford, S. C., … Insel, P. A. (2018). Goals and practicalities of immunoblotting and immunohistochemistry: A guide for submission to the British Journal of Pharmacology. *British Journal of Pharmacology*, *175*, 407–411. https://doi.org/10.1111/bph.14112

Ambati, R. R., Phang, S. M., Ravi, S., & Aswathanarayana, R. G. (2014). Astaxanthin: Sources, extraction, stability, biological activities and its commercial applications--a review[J]. *Marine Drugs*, *12*, 128–152.

Baburina, Y., Krestinin, R., Odinokova, I., Sotnikova, L., Kruglov, A., & Krestinina, O. (2019). Astaxanthin inhibits mitochondrial permeability transition pore opening in rat heart mitochondria. *Antioxidants (Basel)*, *8*, 576–591.

Badman, M. K., Pissios, P., Kennedy, A. R., Koukos, G., Flier, J. S., & Maratos-Flier, E. (2007). Hepatic fibroblast growth factor 21 is regulated by PPARα and is a key mediator of hepatic lipid metabolism in ketotic states. *Cell Metabolism*, *5*, 426–437.

Bailey, S., Robinson, G., Pinner, A., Chamlee, L., Johnson, M., Nagy, T., & Abrams, G. (2005). Mitochondrial dysfunction and NASH in response to a high-fat diet in mice: A functional proteomics approach. *Hepatology*, *42*, 630a–631a.

Baker, P. R., & Friedman, J. E. (2018). Mitochondrial role in the neonatal predisposition to developing nonalcoholic fatty liver disease. *The Journal of Clinical Investigation*, *128*, 3692–3703. https://doi.org/10.1172/JCI120846

Begriche, K., Igoudjil, A., Pessayre, D., & Fromenty, B. (2006). Mitochondrial dysfunction in NASH: Causes, consequences and possible means to prevent it. *Mitochondrion*, *6*, 1–28. https://doi.org/10.1016/j.mito.2005.10.004

Boström, P., Wu, J., Jedrychowski, M. P., Korde, A., Ye, L., Lo, J. C., … Kajimura, S. (2012). A PGC1-α-dependent myokine that drives brown-fat-like development of white fat and thermogenesis. *Nature*, *481*, 463–468. https://doi.org/10.1038/nature10777

Brendler, T., & Williamson, E. M. (2019). Astaxanthin: How much is too much? A safety review. *Phytotherapy Research*, *33*, 3090–3111. https://doi.org/10.1002/ptr.6514

Chen, M. Z., Chang, J. C., Zavala-Solorio, J., Kates, L., Thai, M., Ogasawara, A., … Sonoda, J. (2017). FGF21 mimetic antibody stimulates UCP1-independent brown fat thermogenesis via FGFR1/βKlotho complex in non-adipocytes. *Mol Metab*, *6*, 1454–1467. https://doi.org/10.1016/j.molmet.2017.09.003

Chen, Z., Yu, R., Xiong, Y., Du, F., & Zhu, S. (2017). A vicious circle between insulin resistance and inflammation in nonalcoholic fatty liver disease. *Lipids in Health and Disease*, *16*, 203–211. https://doi.org/10.1186/s12944-017-0572-9

Curtis, M. J., Alexander, S., Cirino, G., Docherty, J. R., George, C. H., Giembycz, M. A., … MacEwan, D. J. (2018). Experimental design and analysis and their reporting II: Updated and simplified guidance for authors and peer reviewers. *Br J Pharmacology*, *175*, 987–993. https://doi.org/10.1111/bph.14153

Czabotar, P. E., Lessene, G., Strasser, A., & Adams, J. M. (2014). Control of apoptosis by the BCL-2 protein family: Implications for physiology and therapy. *Nature Reviews. Molecular Cell Biology*, *15*, 49–63. https://doi.org/10.1038/nrm3722

Day, C. P., & James, O. F. (1998). Steatohepatitis: A tale of two "hits"? *Gastroenterology*, *114*, 842–845. https://doi.org/10.1016/S0016-5085(98)70599-2

Fisher, F. M., Kleiner, S., Douris, N., Fox, E. C., Mepani, R. J., Verdeguer, F., … Spiegelman, B. M. (2012). FGF21 regulates PGC-1α and browning of white adipose tissues in adaptive thermogenesis. *Genes & Development*, *26*, 271–281. https://doi.org/10.1101/gad.177857.111

Fisher, F. M., & Maratos-Flier, E. (2016). Understanding the physiology of FGF21. *Annual Review of Physiology*, *78*, 223–241. https://doi.org/10.1146/annurev-physiol-021115-105339

Gallardo-Montejano, V. I., Saxena, G., Kusminski, C. M., Yang, C., McAfee, J. L., Hahner, L., … Bickel, P. E. (2016). Nuclear Perilipin 5 integrates lipid droplet lipolysis with PGC-1α/SIRT1-dependent transcriptional regulation of mitochondrial function. *Nature Communications*, *7*, 12723–12736. https://doi.org/10.1038/ncomms12723

Garcia-Monzón, C., Martín-Pérez, E., Iacono, O. L., Fernández-Bermejo, M., Majano, P. L., Apolinario, A., … Moreno-Otero (2000). Characterization of pathogenic and prognostic factors of non-alcoholic steatohepatitis associated with obesity. *Journal oJ Hepatology*, *33*, 716–724. https://doi.org/10.1016/S0168-8278(00)80301-3

Gimeno, R. E., & Moller, D. E. (2014). FGF21-based pharmacotherapy–potential utility for metabolic disorders. *Trends in Endocrinology and Metabolism*, *25*, 303–311. https://doi.org/10.1016/j.tem.2014.03.001

Hu, Q., Wang, C., Liu, F., He, J., Wang, F., Wang, W., & You, P. (2019). High serum levels of FGF21 are decreased in bipolar mania patients during

psychotropic medication treatment and are associated with increased metabolism disturbance. *Psychiatry Research*, *272*, 643–648.

Jia, Y., Wu, C., Kim, J., Kim, B., & Lee, S. J. (2016). Astaxanthin reduces hepatic lipid accumulations in high-fat-fed C57BL/6J mice via activation of peroxisome proliferator-activated receptor (PPAR) α and inhibition of PPAR gamma and Akt. *The Journal of Nutritional Biochemistry*, *28*, 9–18. https://doi.org/10.1016/j.jnutbio.2015.09.015

Kang, D., Kim, S. H., & Hamasaki, N. (2007). Mitochondrial transcription factor A (TFAM): Roles in maintenance of mtDNA and cellular functions. *Mitochondrion*, *7*, 39–44. https://doi.org/10.1016/j.mito.2006.11.017

Kelly, D. P., & Scarpulla, R. C. (2004). Transcriptional regulatory circuits controlling mitochondrial biogenesis and function. *Genes & Development*, *18*, 357–368. https://doi.org/10.1101/gad.1177604

Kharitonenkov, A., & DiMarchi, R. (2015). FGF21 revolutions: Recent advances illuminating FGF21 biology and medicinal properties. *Trends in Endocrinology and Metabolism*, *26*, 608–617. https://doi.org/10.1016/j.tem.2015.09.007

Kharitonenkov, A., Dunbar, J. D., Bina, H. A., Bright, S., Moyers, J. S., Zhang, C., … Hale, J. E. (2008). FGF-21/FGF-21 receptor interaction and activation is determined by βKlotho. *Journal of Cellular Physiology*, *215*, 1–7. https://doi.org/10.1002/jcp.21357

Kilkenny, C., Browne, W., Cuthill, I. C., Emerson, M., & Altman, D. G. (2010). Animal research: Reporting in vivo experiments: the ARRIVE guidelines. *British Journal of Pharmacology*, *160*, 1577–1579. https://doi.org/10.1111/j.1476-5381.2010.00872.x

Kim, B., Farruggia, C., Ku, C. S., Pham, T. X., Yang, Y., Bae, M., … Koo, S. I. (2017). Astaxanthin inhibits inflammation and fibrosis in the liver and adipose tissue of mouse models of diet-induced obesity and non-alcoholic steatohepatitis. *The Journal of Nutritional Biochemistry*, *43*, 27–35. https://doi.org/10.1016/j.jnutbio.2016.01.006

Kumar, D. P., Santhekadur, P. K., Seneshaw, M., Mirshahi, F., Uram-Tuculescu, C., & Sanyal, A. J. (2019). A regulatory role of apoptosis antagonizing transcription factor in the pathogenesis of nonalcoholic fatty liver disease and hepatocellular carcinoma. *Hepatology*, *69*, 1520–1534. https://doi.org/10.1002/hep.30346

Lehtonen J. M., Forsström, S., Bottani, E., Isoniemi H., Viscomi C., Barris O. R, Suomalainen, A. (2016). FGF21 is a biomarker for mitochondrial translation and mtDNA maintenance disorders. *Neurology*, *87*(22), 2290–2299. https://doi.org/10.1212/wnl.0000000000003374

Leone, T. C., Lehman, J. J., Finck, B. N., Schaeffer, P. J., Wende, A. R., Boudina, S., … Chen, Z. (2005). PGC-1α deficiency causes multi-system energy metabolic derangements: Muscle dysfunction, abnormal weight control and hepatic steatosis. *PLoS Biology*, *3*(4), 672–687.

Li, H., Fang, Q., Gao, F., Fan, J., Zhou, J., Wang, X., … Xu, A. (2010). Fibroblast growth factor 21 levels are increased in nonalcoholic fatty liver disease patients and are correlated with hepatic triglyceride. *Journal of Hepatology*, *53*, 934–940.

Li, R., Xin, T., Li, D., Wang, C., Zhu, H., & Zhou, H. (2018). Therapeutic effect of Sirtuin 3 on ameliorating nonalcoholic fatty liver disease: The role of the ERK-CREB pathway and Bnip3-mediated mitophagy. *Redox Biology*, *18*, 229–243.

Liu, H., Liu, H., Zhu, L., Zhang, Z., Zheng, X., Liu, J., & Fu, X. (2016). Hepatic oleate regulates liver stress response partially through PGC-1α during high-carbohydrate feeding. *Journal of Hepatology*, *65*, 103–112. https://doi.org/10.1016/j.jhep.2016.03.001

Liu, H., Liu, H., Zhu, L., Zhang, Z., Zheng, X., Liu, J., & Fu, X. (2019). Comparative transcriptome analyses provide potential insights into the molecular mechanisms of astaxanthin in the protection against alcoholic liver disease in mice. *Marine Drugs*, *17*, 181–193.

Lustig, Y., Ruas, J. L., Estall, J. L., Lo, J. C., Devarakonda, S., Laznik, D., … Spiegelman, B. M. (2011). Separation of the gluconeogenic and mitochondrial functions of PGC-1α through S6 kinase. *Genes & Development*, *25*, 1232–1244. https://doi.org/10.1101/gad.2054711

Mao, Y., Cheng, J., Yu, F., Li, H., Guo, C., & Fan, X. (2015). Ghrelin attenuated lipotoxicity via autophagy induction and nuclear factor-κB inhibition. *Cellular Physiology and Biochemistry*, *37*, 563–576. https://doi.org/10.1159/000430377

Miele, L., Forgione, A., Gasbarrini, G., & Grieco, A. (2007). Noninvasive assessment of fibrosis in non-alcoholic fatty liver disease (NAFLD) and non-alcoholic steatohepatitis (NASH). *Translational Research*, *149*, 114–125. https://doi.org/10.1016/j.trsl.2006.11.011

Monmeesil, P., Fungfuang, W., Tulayakul, P., & Pongchairerk, U. (2019). The effects of astaxanthin on liver histopathology and expression of superoxide dismutase in rat aflatoxicosis. *The Journal of Veterinary Medical Science*, *81*, 1162–1172. https://doi.org/10.1292/jvms.18-0690

Montesano, A., Senesi, P., Vacante, F., Mollica, G., Benedini, S., Mariotti, M., … Terruzzi, I. (2019). L-Carnitine counteracts in vitro fructose-induced hepatic steatosis through targeting oxidative stress markers. *Journal of Endocrinological Investigation*, 493–503.

Ni, Y., Nagashimada, M., Zhuge, F., Zhan, L., Nagata, N., Tsutsui, A., … Ota, T. (2015). Astaxanthin prevents and reverses diet-induced insulin resistance and steatohepatitis in mice: A comparison with vitamin E. *Scientific Reports*, *5*, 17192–17206.

Pai, S. A., Munshi, R. P., Panchal, F. H., Gaur, I. S., & Juvekar, A. R. (2019). Chrysin ameliorates nonalcoholic fatty liver disease in rats. *Naunyn-Schmiedeberg's Archives of Pharmacology*, *392*, 1617–1628. https://doi.org/10.1007/s00210-019-01705-3

Pai, S. A., Munshi, R. P., Panchal, F. H., Gaur, I. S., Mestry, S. N., Gursahani, M. S., & Juvekar, A. R. (2019). Plumbagin reduces obesity and nonalcoholic fatty liver disease induced by fructose in rats through regulation of lipid metabolism, inflammation and oxidative stress. *Biomedicine & Pharmacotherapy*, *111*, 686–694. https://doi.org/10.1016/j.biopha.2018.12.139

Piccinin, E., & Moschetta, A. (2016). Hepatic-specific PPARα-FGF21 action in NAFLD. *Gut*, *65*, 1075–1076. https://doi.org/10.1136/gutjnl-2016-311408

Piccinin, E., Villani, G., & Moschetta, A. (2019). Metabolic aspects in NAFLD, NASH and hepatocellular carcinoma: The role of PGC1 coactivators. *Nature Reviews. Gastroenterology & Hepatology*, *16*, 160–174. https://doi.org/10.1038/s41575-018-0089-3

Potthoff, M. J. (2017). FGF21 and metabolic disease in 2016: A new frontier in FGF21 biology. *Nature Reviews. Endocrinology*, *13*, 74–76. https://doi.org/10.1038/nrendo.2016.206

Potthoff, M. J., Inagaki, T., Satapati, S., Ding, X., He, T., Goetz, R., … Burgess, S. C. (2009). FGF21 induces PGC-1α and regulates carbohydrate and fatty acid metabolism during the adaptive starvation response. *PNAS*, *106*, 10853–10858. https://doi.org/10.1073/pnas.0904187106

Recena Aydos, L., Aparecida do Amaral, L., Serafim de Souza, R., Jacobowski, A. C., Freitas dos Santos, E., & Rodrigues Macedo, M. L. (2019). Nonalcoholic fatty liver disease induced by high-fat diet in C57bl/6 models. *Nutrients*, (*12*), 3067–3078. https://doi.org/10.1039/nu11123067

Scarpulla, R. C. (2008). Transcriptional paradigms in mamalian mitochondrial biogenesis and function. *Physiological Reviews*, *88*, 611–638. https://doi.org/10.1152/physrev.00025.2007

Schuppan, D., Surabattula, R., & Wang, X. Y. (2018). Determinants of fibrosis progression and regression in NASH. *Journal of Hepatology*, *68*, 238–250. https://doi.org/10.1016/j.jhep.2017.11.012

Schwabe, R. F., & Luedde, T. (2018). Apoptosis and necroptosis in the liver: A matter of life and death. *Nature Reviews. Gastroenterology & Hepatology*, *15*, 738–752. https://doi.org/10.1038/s41575-018-0065-y

Sharma, M., Vikram, N. K., Misra, A., Bhatt, S., Tarique, M., Parray, H. A., … Luthra, K. (2013). Assessment of 11-β hydroxysteroid dehydrogenase (11-βHSD1) 4478T>G and tumor necrosis factor-α (TNF-α)-308G>A

polymorphisms with obesity and insulin resistance in Asian Indians in North India. *Molecular Biology Reports*, *40*, 6261–6270. https://doi.org/10.1007/s11033-013-2738-5

Tilg, H., Moschen, A. R., & Szabo, G. (2016). Interleukin-1 and inflammasomes in alcoholic liver disease/acute alcoholic hepatitis and nonalcoholic fatty liver disease/nonalcoholic steatohepatitis. *Hepatology*, *64*, 955–965. https://doi.org/10.1002/hep.28456

Virbasius, J. V., & Scarpulla, R. C. (1994). Activation of the human mitochondrial transcription factor A gene by nuclear respiratory factors: A potential regulatory link between nuclear and mitochondrial gene expression in organelle biogenesis. *Proceedings of the National Academy of Sciences of the United States of America*, *91*, 1309–1313. https://doi.org/10.1073/pnas.91.4.1309

Wang, L., Liu, X., Nie, J., Zhang, J., Kimball, S. R., Zhang, H., … Shi, Y. (2015). ALCAT1 controls mitochondrial etiology of fatty liver diseases, linking defective mitophagy to steatosis. *Hepatology*, *61*, 486–496. https://doi.org/10.1002/hep.27420

Williamson, E. M., Liu, X., & Izzo, A. A. (2020). Trends in use, pharmacology, and clinical applications of emerging herbal nutraceuticals. *British Journal of Pharmacology*, *177*, 1227–1240. https://doi.org/10.1111/bph.14943

Yan, W., Zhang, H., Liu, P., Wang, H., Liu, J., Gao, C., … Tao, L. (2013). Impaired mitochondrial biogenesis due to dysfunctional adiponectin-AMPK-PGC-1α signaling contributing to increased vulnerability in diabetic heart. *Basic Research in Cardiology*, *108*, 329–343. https://doi.org/10.1007/s00395-013-0329-1

Yan, X., Chen, J., Zhang, C., Zhou, S., Zhang, Z., Chen, J., … Tan, Y. (2015). FGF21 deletion exacerbates diabetic cardiomyopathy by aggravating cardiac lipid accumulation. *Journal of Cellular and Molecular Medicine*, *19*, 1557–1568. https://doi.org/10.1111/jcmm.12530

Zhou, H., Du, W., Li, Y. E., Shi, C., Hu, N., Ma, S., … Ren, J. (2018). Effects of melatonin on fatty liver disease: The role of NR4A1/DNA-PKcs/-p53 pathway, mitochondrial fission, and mitophagy. *Journal of Pineal Research*, *64*. https://doi.org/10.1111/jpi.12450

## SUPPORTING INFORMATION

Additional supporting information may be found online in the Supporting Information section at the end of this article.

**How to cite this article:** Wu L, Mo W, Feng J, et al. Astaxanthin attenuates hepatic damage and mitochondrial dysfunction in non-alcoholic fatty liver disease by up-regulating the FGF21/PGC-1α pathway. *Br J Pharmacol*. 2020; 177:3760–3777. https://doi.org/10.1111/bph.15099